Netherlands Journal of Sea Research
25 (3): 351-364 (1990)

OBSERVATIONS OF PHYSICAL AND BIOLOGICAL PARAMETERS AT THE TRANSITION BETWEEN THE SOUTHERN AND CENTRAL NORTH SEA

J.J.M. VAN HAREN and J.C.A. JOORDENS
Netherlands Institute for Sea Research, P.O. Box 59, 1790 AB Den Burg, Texel, The Netherlands

ABSTRACT

In the area between the 30 and 40 m isobaths, just north of the Netherlands, a transition from Channel water to central North Sea water is found. Observations obtained in May and June 1986 show a predominantly along-isobath directed sub-tidal current. In the vertical cross-isobath plane a quasi-permanent upwelling zone overlying the steepest bottom slope is inferred from observed cross-isobath currents.

In the same area CREUTZBERG (1985) observed a persistent chlorophyll *a* (chl *a*) maximum. Our observations show a chl *a* maximum extending from the bottom towards the pycnocline over a larger area in cross-isobath direction and with larger amounts of chl *a* than found by CREUTZBERG (1985). This chl *a* maximum is found above a zone of large amounts of benthic particulate organic carbon.

The observed chl *a* distributions are compared with current and density observations via an advection-diffusion equation. Only rough estimates of the terms in this equation are obtained, which indicates that a balance between vertical advection and mixing, *i.e.* local generation, is most probable. The chl *a* distribution gives no evidence for an upwelling zone.

1. INTRODUCTION

CREUTZBERG (1985) has described the existence of a persistent chlorophyll *a* (chl *a*) maximum above a bottom slope, which is rather steep compared with the surrounding bottom topography and which is located between the 30-40 m isobaths at the transition between the southern and central North Sea (Fig. 1). Between these isobaths a transition from sandy to mud-containing sediments is found (Fig. 1b). By considering tidal currents only, CREUTZBERG & POSTMA (1979) have shown that silt and particulate organic matter are kept in suspension in the tidally more energetic southern North Sea and may be deposited in the central North Sea (Fig. 1a). In the mud-containing sediments larger biomass values of the benthic fauna are found (CREUTZBERG *et al.*, 1984), with probably larger associated amounts of nutrients.

On the other hand, it has been shown by PINGREE & GRIFFITHS (1978) that in summer a tidal mixing front overlies the same area. It is commonly accepted that at a (tidal mixing) front, which determines the border between separate water masses containing different amounts of nutrients, enhanced primary production may be found (*e.g.* LODER & PLATT, 1985). A probable mechanism for this enhanced production may be cross-frontal circulation, which is induced by the front (GARRETT & LODER, 1981).

After comparison of chl *a* distributions with temperature observations, CREUTZBERG (1985) concluded that the chl *a* maximum is most probably due to the enriched bottom zone. For this, he assumed that after mineralization nutrients would be mixed with the overlying water mass, thereby favouring phytoplankton growth.

In this paper we present chl *a* distributions observed in May and June 1986 between 53°30′-54°00′ N, 4°10′-4°50′ E. The distributions are compared with data from current meters and CTD-equipment. Some additional data from bird counts and echo-sound scans obtained in different periods are discussed as well. The purpose is to relate the chl *a* distribution with the observed sub-tidal currents, in which case the chl *a* will be considered as a tracer. Secondly, in search of a local relationship between the chl *a* maximum and the enriched benthic zone, vertical mixing is considered.

In the following, horizontal mixing will not be taken into account. A linear relationship will be assumed between chl *a* content and biomass. Possible effects such as the higher chl *a* content per cell in light-limited zones (noted by CULLEN, 1982) and the differing chl *a* content for different phytoplankton species are ignored. Also, grazing by herbivores is not considered.

To compare our data with the observations of CREUTZBERG (1985), the latter have been replotted in

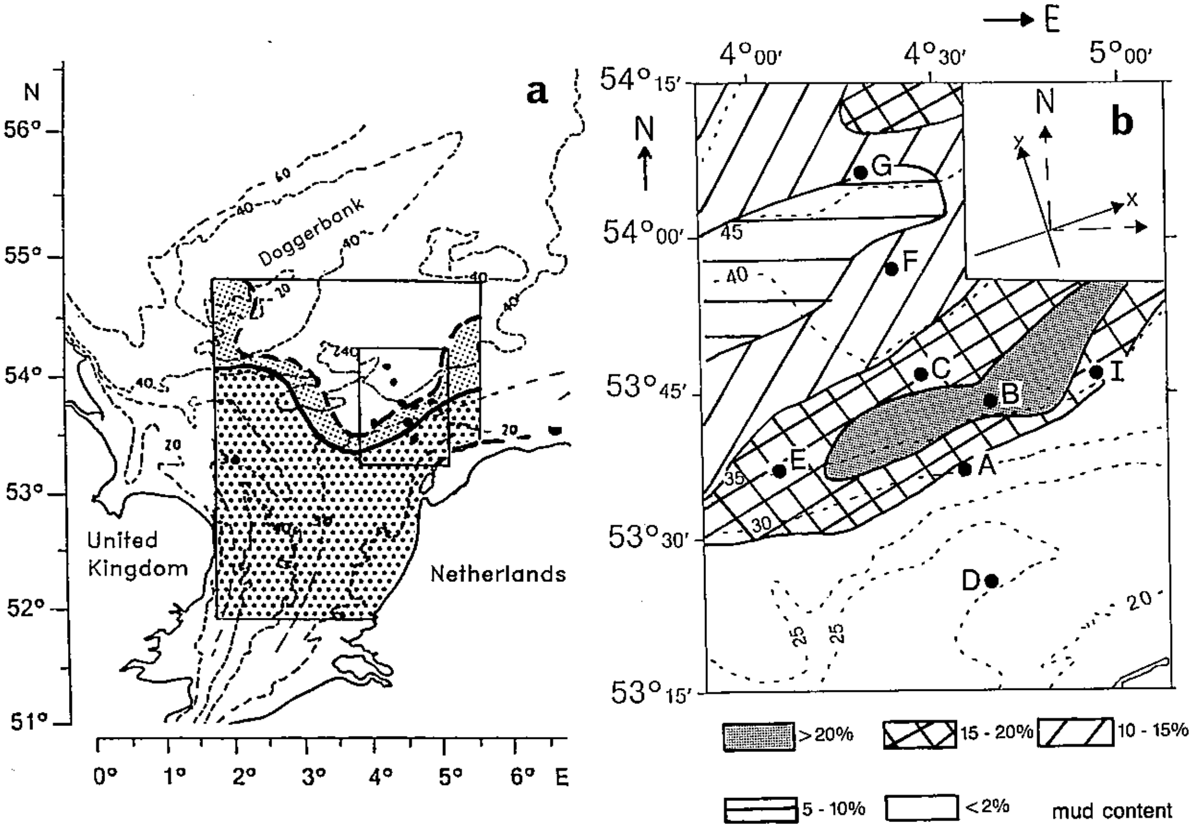

Fig. 1a. Southern part of the North Sea with the investigation area marked by the small rectangle. The 'theoretical' silt chart is redrawn from CREUTZBERG & POSTMA (1979), with the heavy dotted area denoting 'erosion and turbidity' (no deposition) and white denoting 'no erosion and no turbidity' (deposition). b. Investigation area with isobaths (during LLWS) drawn every 5 m and current meter moorings A-I marked by ●. The distribution of mud content (particles < 50 μm) is redrawn from CREUTZBERG *et al.* (1984). In the upper right-hand corner the directions of the adopted horizontal coordinate axes are shown.

a summarized form in a vertical cross-isobath plane (Fig. 2). The region of distinct large chl *a* contents observed by CREUTZBERG (1985) is here classified in three types and one subtype. Type A (hereafter called TA) is a surface-to-bottom chl *a* maximum of typically 3 mg m^{-3}. It overlies the 15-20% mud content region closest to the top of the bottom slope. This is the chl *a* maximum CREUTZBERG (1985) discusses. The sketched chl *a* distribution of TA' and TB has been observed once by him, at the end of May 1983. CREUTZBERG (1985) attributes the lack of a surface-to-bottom chl *a* maximum (*i.e.* TA) to overlying thermal stratification. Unfortunately, CREUTZBERG (1985) does not dicuss TB with large (>20 mg m^{-3}) chl *a* values. Finally, type C contains large values of chl *a* at the thermocline in deeper waters outside the range of Fig. 2. They will not be dicussed in this paper.

After a description of data handling in Section 2, this paper continues with the relevant physical processes in Section 3. Transport in the horizontal plane will be compared with the distribution of some observables in Section 4, followed by a discussion on the chl *a* distribution in a vertical cross-isobath plane in Section 5.

Acknowledgements.—The pleasant cooperation with the crew of RV 'Aurelia' resulted in a fruitful gathering of data. Additional CTD data and the turbidity data were obtained from RV 'Holland' of the North Sea Division of the Dutch Ministry of Transport and Public Works. Gijs Kraay supplied the HPLC data on pigments and Mardik Leopold the data of bird counts and the echo-sound scan of RV 'Tridens'. Bouwe Kuipers provided the interpretation of echo-sound responses obtained on board RV 'Aurelia'. Leo Maas supported and stimulated us. Loes Gerringa typed the bulk.

J.J.M. van Haren was supported by a grant of the Netherlands Organization for Scientific Research (NWO).

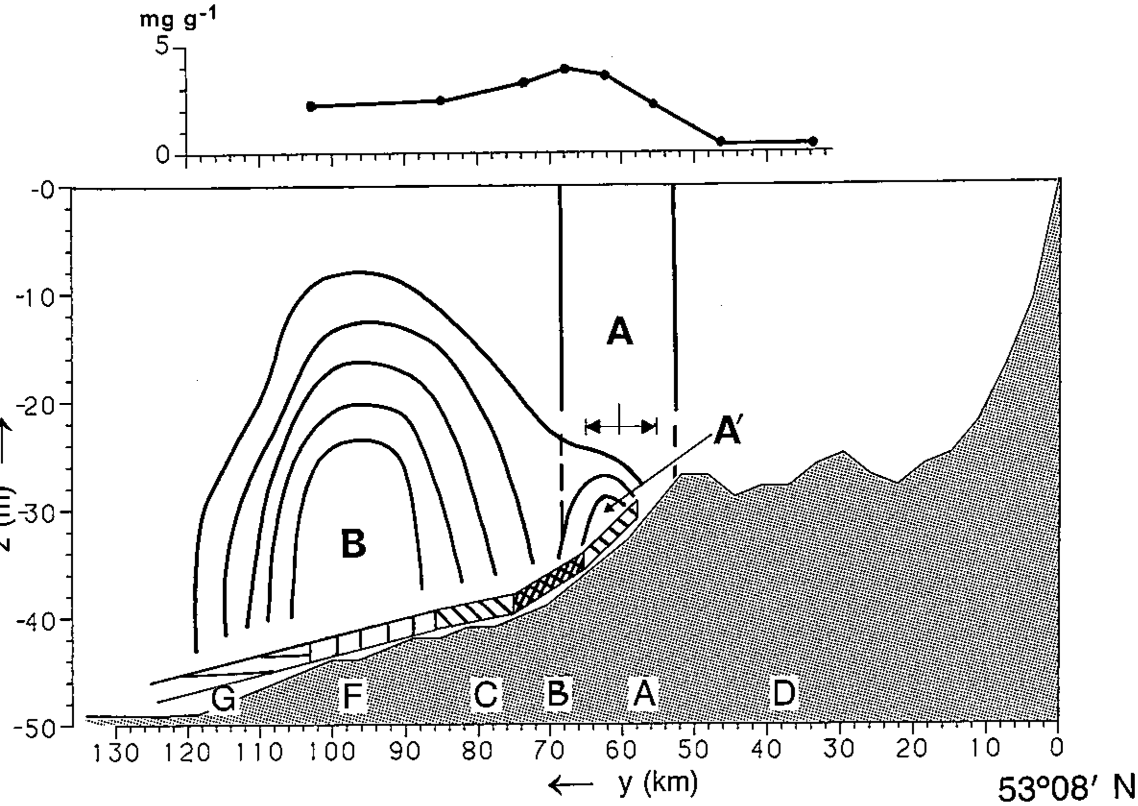

Fig. 2. Summary of chl *a* distributions observed by CREUTZBERG (1985) in a vertical cross-isobath plane along the y-axis. Type A: surface-bottom chl *a* maximum of which the uncertainty in its center position is indicated. Type B and subtype A' have been observed together by CREUTZBERG (1985). Above the diagram the magnitude of particulate organic carbon (POC) content in the bottom is shown in mg g^{-1} (CREUTZBERG, 1985). The origin of the y-axis is located at 53°08′ N, 4°45′ E. The panel following the bottom contour is showing the mud content, with the following legend between moorings A-G: 15-20%, >20%, 15-20%, 10-15%, 5-10%.

2. DATA HANDLING

NBA-DNC 2M (and 2B) current meters have been located at the positions shown in Fig. 1b; wind data have been gathered at platform K_{13}, located at 53°15′ N, 3°15′ E. The positions of the current meters and the periods of observations are given by VAN HAREN (1990a). All time series have been tidally filtered. Only signals with 'sub-tidal' frequencies $\sigma < 0.7$ cpd will be considered. Currents fluctuating with these frequencies include wind-driven currents and density-driven currents. The currents observed ($\vec{u}$ =(u,v)) and wind stresses ($\vec{\tau}$ =(τ_x,τ_y)) have been decomposed along the axes of a right-handed coordinate system, the x-axis of which is directed along the isobaths (Fig. 1b). The origin has been located near the Dutch coast at the sea surface. Typical time series of current and wind stress components are shown in Fig. 3. From every current meter record progessive vector plots have been constructed. In Section 4 these vector plots will be interpreted as particle displacements in the horizontal plane. It should be noted that this interpretation of progessive vector plots is not strictly correct, because the current pattern of the surroundings is not included. Water density observations have been inferred from data obtained with a Neil Brown smart CTD.

At some CTD stations 1-dm^3 water samples have been taken. Each water sample has been filtered over a Whatman GFC glass fibre filter, which was stored frozen. In the laboratory a mixture of each filter, small glass pearls and 10 cm^3 90% acetone has been homogenized. After dilution of the resulting extract with 90% acetone, its fluorescence R_a has been measured with a Turner 111 fluorometer. Next, the extract has been acidified with 0.5 M HCl and

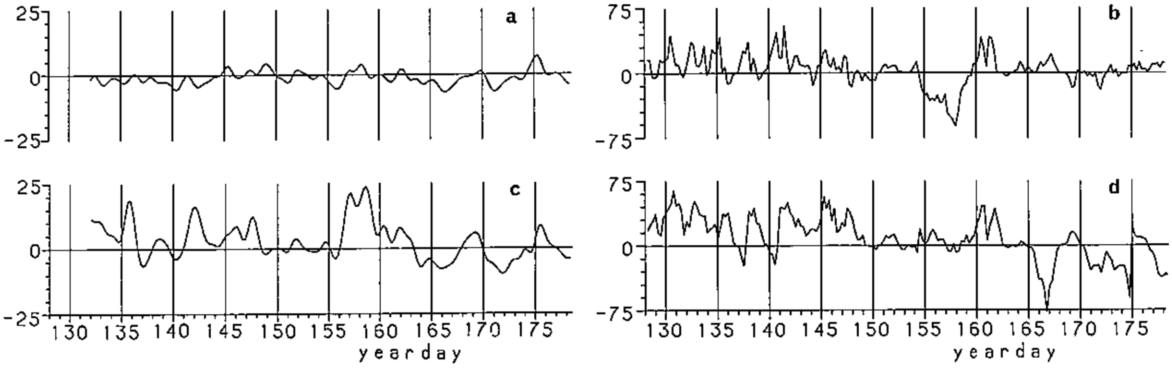

Fig. 3. Sub-tidal time series of currents in cm s^{-1} observed at 11.5 m from the surface at mooring B and wind stresses in 10^{-2} N m^{-2} inferred from observations at K_{13} in May and June 1986 (Day 121=May 1st). a. cross-isobath current component b. cross-isobath wind stress c. along-isobath current component d. along-isobath wind stress.

fluorescence has again been measured, resulting in the value R_b. The difference between R_a and R_b determines the amount of chl *a* and its ratio is called 'acid' ratio $R = R_a/R_b$. If $R > 1.8$ the phytoplankton is considered fresh, as it contains only small amounts of phaeopigments (SIMPSON *et al.*, 1978). Cluster analysis has been performed on 20 algal pigments from the spectral distribution obtained by HPLC.

High resolution echo-sound scans have been obtained with an ELAC 50 kHz echo-sounder of RV 'Tridens' and a 35 kHz Simrad Scientific echo-sounder of RV 'Aurelia', while sailing along tracks in cross-isobath direction. The characteristic length scales for response at these frequencies point to reflectance on small fish (sprat; *Sprattus sprattus*).

Although currents have little influence on the motion of fish, they probably do follow food supplies carried by the currents. Hence, a good fit may be expected between echo-sound responses and phytoplankton abundance, provided that feeders on the latter (*e.g.* copepods) remain in the same area.

Bird counts have been performed from various vessels crossing the area of study. Only data on the species Guillemot (*Uria aalge*) are considered, which feed on sprat (M.F. Leopold, pers. comm.).

3. PHYSICAL PROCESSES

By considering chl *a* as a tracer, its distribution may be explained by using an advection-diffusion equation. Therefore, knowledge on the currents is required. Before describing this equation, we consider the vertical component of water and particle velocities, which contribute to an important term in this equation.

From the horizontal currents, measured at several positions in the vertical, a vertical water velocity component (w) can be inferred from the continuity equation:

$$w(z) = -\int_{-H}^{z} \left(\frac{\partial u}{\partial x} + \frac{\partial v}{\partial y}\right) dz + w(-H) \;, \qquad (1)$$

with: $w(-H) = \left(u\frac{\partial H}{\partial x} + v\frac{\partial H}{\partial y}\right)\Big|_{z=-H}$

The near-bottom vertical velocity $w(-H)$ is generally small. In a 'convergence', $(\partial u/\partial x + \partial v/\partial y)$ is negative and hence a positive w is found: 'upwelling'. VAN HAREN (1990b) has found a quasi-permanent upwelling region between moorings A and B (see also Section 5). In this region, typical values of w range between $0.4 \cdot 10^{-2} < w < 1.2 \cdot 10^{-2}$ cm s^{-1} ($3.5 < w < 10$ m day^{-1}).

Phytoplankton and sediment particles have negative buoyancy. Their settling velocity w_s can be described in simplified form by Stokes' law:

$$w_s = \frac{-gd^2\Delta\varrho}{18\eta} \;, \qquad (2)$$

in which $\Delta\varrho$ denotes the density difference between a particle and the surrounding water, η the (temperature-dependent) dynamic viscosity ($\eta_{20^\circ C}$ = 10^{-3} kg m^{-1} s^{-1}), g = 9.81 m^2 s^{-1} the acceleration of gravity and d the diameter of the particle. Stokes' law is valid for spherical particles in viscous flow.

For colloids and flocs MCCAVE (1984) gives a number of settling velocities according to (2) for different particle diameters, by using a relationship between $\Delta\varrho$ and d: d=20 μm: $w_s = -0.4 \cdot 10^{-2}$ cm s^{-1}; d=50 μm: $w_s = -1.7 \cdot 10^{-2}$ cm s^{-1}; d=200 μm: $w_s = -4.6 \cdot 10^{-2}$ cm s^{-1}.

Phytoplankton particles have a wide range of sizes between O(1 μm) and O(10^3 μm). BIENFANG (1980) estimates w_s from ship-laboratory experiments using a settling column as: $w_s \approx -(0.09-0.18) \pm 0.02 \cdot 10^{-2}$ cm s^{-1} for phytoplankton with $3 < d < 120$ μm.

SMETACEK *et al.* (1978) estimate w_s for diatoms from sediment trap catches as $w_s \approx -0.92\cdot10^{-2}$ cm s^{-1}. As we have not observed w_s (or $\Delta\varrho$) for phytoplankton particles during our study, we have to rely on estimates from the literature as given above. The magnitudes of w_s given are of the same order as w and the latter may thus considerably influence the vertical movement of phytoplankton in restricted areas.

When the current field is known, the relative importance of advection by sub-tidal currents and vertical turbulent mixing, induced by tidal currents via bottom stress and by wind stress at the sea surface, can be inferred from the distribution of the concentration (C) of suspended particles by assuming that its steady state is described by an advection-diffusion equation:

$$u\frac{\partial C}{\partial x}+v\frac{\partial C}{\partial y}+(w+w_s)\frac{\partial C}{\partial z}=\frac{\partial}{\partial z}(K_d\frac{\partial C}{\partial z})+(G-L)\ , \qquad (3)$$

in which K_d denotes the turbulent vertical eddy diffusivity. The last term in the right-hand side of (3) denotes the local (G)eneration and (L)oss processes.

If we ignore this last term, a value of K_d is needed before the validity of (3) can be verified with observations. It is difficult to estimate K_d directly. However, in well-mixed water $K_d \approx K_z$, with K_z the turbulent vertical eddy viscosity which is used for parametrization of the vertical turbulent momentum transfer. According to CSANADY (1982), the latter can be estimated as:

$$K_z=\frac{u_*H}{16}\ , \qquad (4)$$

with $u_*=(r'U)^{0.5}$, r' a bottom friction parameter, U the (tidal) current amplitude and $f = 1.175\cdot10^{-4}$ s^{-1} the Coriolis parameter. From the vertical sub-tidal current structure VAN HAREN (1990b) finds reasonable agreement between the observed and modelled vertical current structure for $K_z=25\cdot10^{-3}$ m^2 s^{-1}.

Stratification reduces K_z, typically to 10% of the value given above (VAN HAREN, 1990b) and enhances the vertical current shear. The ratio K_d/K_z is dependent on the stratification rate and the vertical current shear:

$$\frac{K_d}{K_z}=F(Ri)\ , \qquad (5)$$

with: $Ri=(-\frac{g}{\varrho}\frac{\partial\varrho}{\partial z})\cdot(\frac{\partial A}{\partial z})^{-2}=N^2\cdot(\frac{\partial A}{\partial z})^{-2}$

the Richardson number, ϱ the density of sea water, N the Brunt-Väisälä frequency and A the total, *i.e.* tidal and sub-tidal, current amplitude. Many descriptions of F(Ri) exist (ABRAHAM, 1988), but they all show a rapid decrease of K_d/K_z for increasing Ri. For a typical mooring C the total current shear is estimated as $\partial A/\partial z = 1.4\cdot10^{-2}$ s^{-1} (MAAS & VAN HAREN (1987) for the tidal current profile and VAN HAREN (1990a) for the sub-tidal current profile) and $N \approx 10^{-2}$ s^{-1}, yielding (Fig. 6 given by ABRAHAM, 1988) $Ri\approx0.5$ and $K_d\approx0.2\cdot K_z$. In a stratified layer the values of $\partial A/\partial z$ and N are estimated as $4\cdot10^{-2}$ s^{-1}, which gives $Ri\approx1$, $K_d\approx0.1\cdot K_z$. Hence, values of K_d are estimated as: $K_d\approx5\cdot10^{-3}$ m^2 s^{-1} for surface and bottom 'nearly-mixed' layers and $K_d\approx0.2\cdot10^{-3}$ m^2 s^{-1} in the pycnocline (in which $K_z\approx2\cdot10^{-3}$ m^2 s^{-1}). It is stressed that considering the crudeness of the estimates, the given values are indicative only.

Nevertheless, separate terms in (3) will be estimated in Section 5. First a description of the distribution of several observations in the horizontal plane will be given in the next section.

4. OBSERVATIONS IN THE HORIZONTAL PLANE

In September 1985 the area was extensively scanned by the echo-sounder on board RV 'Aurelia' (Fig. 4a). Non-zero response was found between 12-17 m depth, extending over a narrow band (width ≈ 6 km) along the southern rim of the area with the largest mud content. Outside the region displayed, no distinctive responses have been found (the observations were carried out between 3° and 6° E, Kuipers, pers. comm.). Thus, response was not found along the total area of mud content > 15% (Fig. 1b). The width and the position of the area of non-zero response correspond closely to the width and position of TA chl *a* maximum, observed by CREUTZBERG (1985).

The distribution of non-zero echo-sound response was found in the same area as the abundance of Guillemot, which was observed between days 210-212 in 1987 (Fig. 4b). This distribution was found throughout August 1987 (LEOPOLD, 1988). Like the extent of the echo-sound responses, the extent of large numbers of birds in along-isobath direction was small, although larger than in cross-isobath direction.

The shape of the distribution of near-surface turbidity, observed during the same period (210-212, 1987), points to a source lying WSW of the area displayed in Fig. 4c. Due to lack of calibration, the formazine turbidity units (FTU) cannot be transferred to a more useful sediment concentration. Nevertheless, if FTU > 2.0 is assumed as high turbidity, the area overlaid with turbid water was considerably larger than the area in which larger numbers of Guillemot were observed.

It is acknowledged that two sources may contribute to the deposition of mud in our area: one is the Rhine estuary and the other lies off the East-Anglian coast, from the Thames estuary towards the Wash

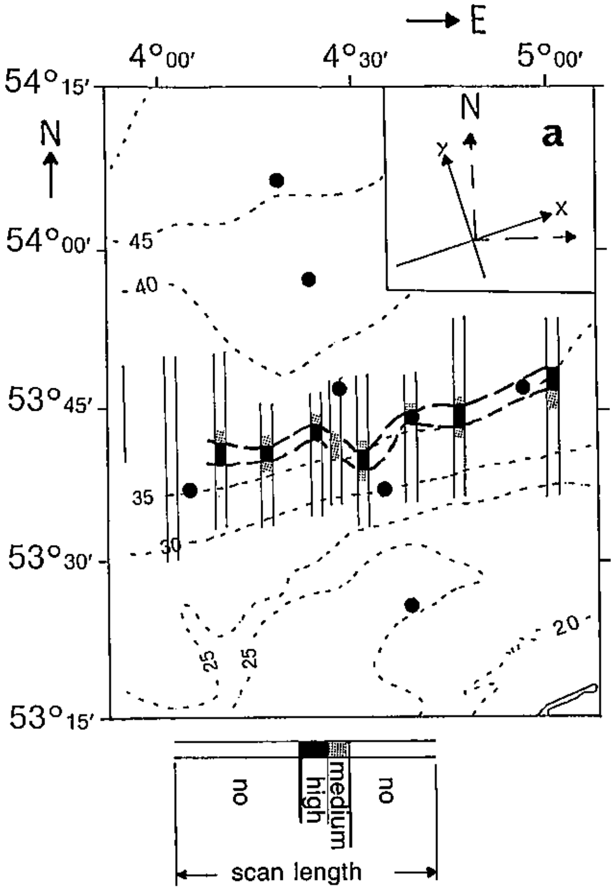

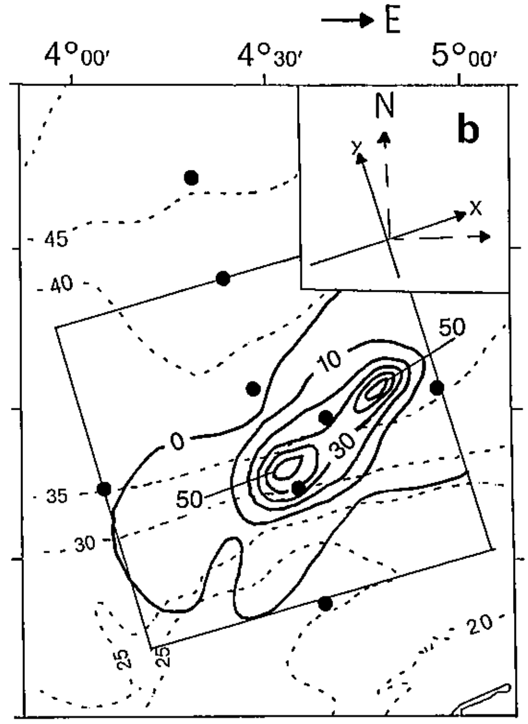

Fig. 4. Horizontal distributions of several parameters. a. Interpretation in three grey tones of 35 kHz echo-sounder scans observed in September 1985. b. Numbers per 10 km of Guillemot observed within a distance of ±300 m from the ship between days 210-212, 1987 along transects parallel to the y-axis and separated 10 km. c. Surface turbidity in Formazine Turbidity Units observed between days 210-212, 1987.

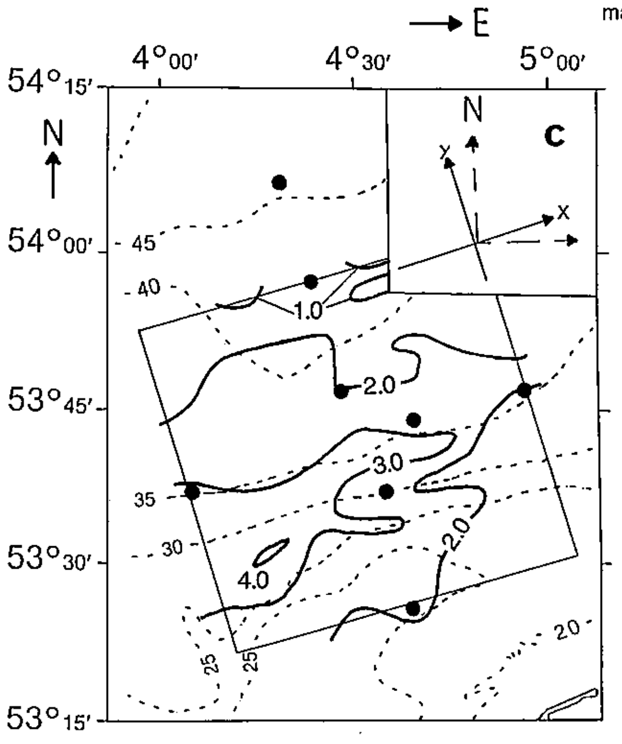

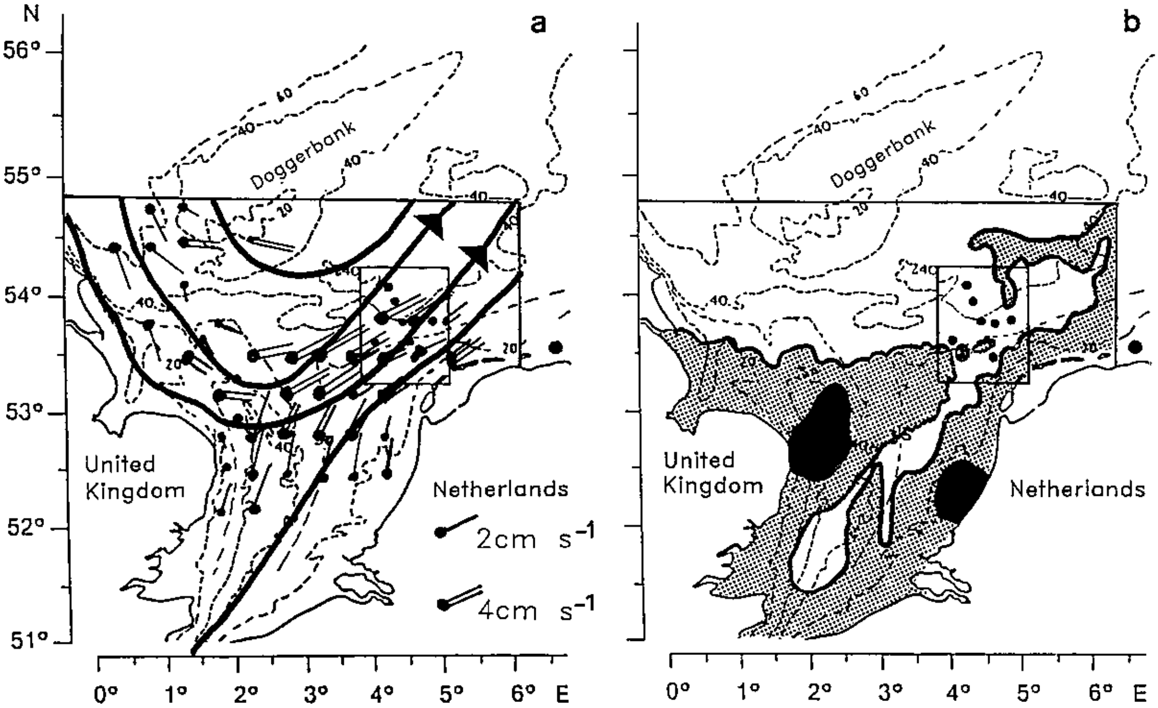

Fig. 5a. Monthly averaged currents and streamlines from a numerical model, developed by PRANDLE (1984). b. 'chl *a*' distribution inferred from CZCS-data obtained on day 166, 1986, redrawn from HOLLIGAN *et al.* (1989). Darker shades indicate larger amounts of 'chl *a*'. Note the remarks on the interpretation of this Fig. in the text.

and centred near the Norfolk Banks (53° N, 2° E) (EISMA & KALF, 1987). It is difficult to establish which source contributes most: a comparison of maps on the residual current pattern in the North Sea gives no decisive answer. They certainly indicate that our area is a delicate transition zone in which Central North Sea, English Coastal, Channel and Continental Coastal waters meet. Recently developed hydrodynamic models (*e.g.* PINGREE & GRIFFITHS, 1980; Fig. 5a is taken from PRANDLE, 1984) show that under average wind conditions the Rhine outflow closely follows the Dutch coast and that particles released near the Norfolk Banks enter our area.

This 'result' is confirmed by CZCS (Coastal Zone Color Scanner) channel 3 images of reflectance at 550 nm obtained from the Nimbus-7 satellite (HOLLIGAN *et al.*, 1989). A sediment-rich plume is observed on 5 out 7 cloud-free images, which are displayed by HOLLIGAN *et al.* (1989). It extends from the Norfolk Banks towards our area. HOLLIGAN *et al.* (1989) also give distributions on chl *a*, which they have deduced from the CZCS-data by using one algorithm. Unfortunately, they remark that in the turbid waters their chl *a* values may be unreliable, though they do not mention to what extent. However, their 'chl *a*' distribution is essentially similar to their channel 3 reflectance images, *i.e.* a band of chl *a* extending from the Norfolk Banks and ending in, or overlying, a narrow zone, our area (Fig. 5b).

Thus, together with mud and probably detritus, possibly also chl *a* is transported from the Norfolk Banks towards our area. Although no quantitative information can be deduced from the CZCS images, this hypothesis is compared to local generation in the next section.

5. DISTRIBUTIONS IN A VERTICAL CROSS-ISOBATH PLANE

The local sub-tidal current is generally directed along the isobaths (Fig. 6a). Between days 133-160 in 1986, with prevailing SW-winds up to day 155 and a NW storm between 155-160, a particle may have travelled a distance of 115 km (at an average speed of 4.9 cm s^{-1}), which approximates the distance between the Norfolk Banks and our area ($\approx$150 km). If a sloping front overlies the steep bottom slope in the vertical cross-isobath plane, an additional along-isobath current component of 2.5 cm s^{-1} is found (VAN HAREN, 1990b). Thus, at this particular position (mooring A) the along-isobath residual transport may be 1.5 times larger than in its surroundings. This enlargement is

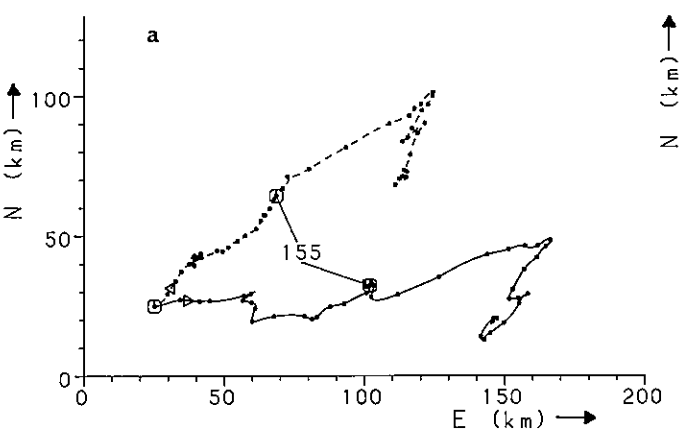

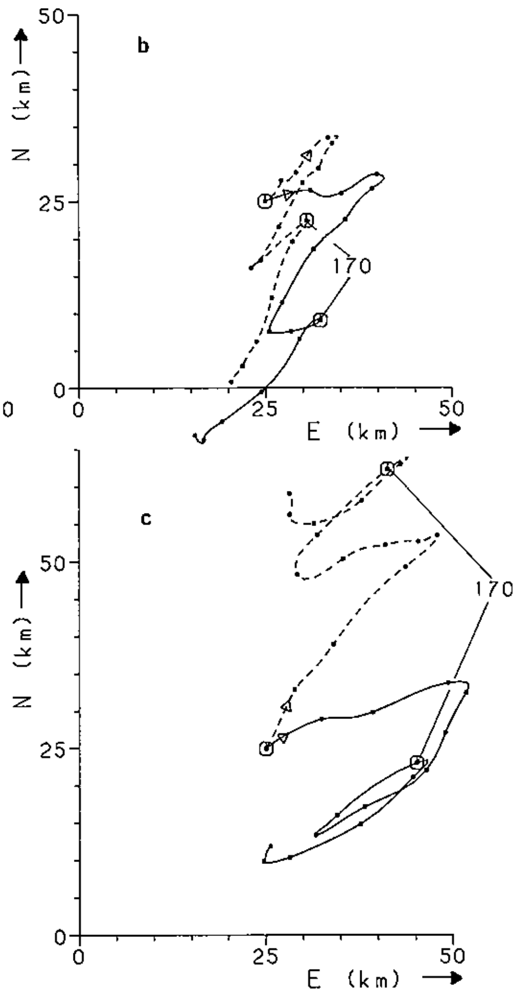

Fig. 6. Progressive vectorplots calculated from sub-tidal currents. Dots represent days. In every plot an arbitrary origin is located at (E,N)=(25,25) km. The axes only denote the direction of the coordinates 'East' and 'North', not their values. a. Total measurement period between May 13 (day 133) and June 28 (day 179) in 1986 for mooring B. Data from the current meter at 11.5 m from the surface are represented by a solid line and those from 8.5 m from the bottom by a dashed line. b. Similar as (a) but for the period June 9-24. c. Similar as (b) but for mooring A: 14.5 m from the surface (solid) and 5.5 m from the bottom (dashed).

not resolved by numerical models; the above mentioned value of 4.9 cm s^{-1} corresponds to the values given by PRANDLE (1984) (Fig. 5a).

Between days 160-175 the wind stress and the current components change direction every 3-5 days (Fig. 3, Figs 6b-c). The water seems to be 'trapped' locally.

5.1. MAY 1986

Due to rough weather conditions only few observations of density and chl *a* were obtained in May 1986. Indicative of the variability in time are the two chl *a* distributions observed on day 146 (Fig. 7a; strong SW winds) and day 149 (Fig. 7b; calm weather). Clearly, large amounts of chl *a* are observed over the large mud-content zone, but a subsurface maximum is found on day 146 and a near-bottom maximum is found on day 149. The density distribution shows a weak front between moorings A-B and a weak pycnocline extending at an average depth of 10 m (Fig. 7c). The chl *a* distribution (day 149) is bounded by this frontal zone and the pycnocline. Results from cluster analysis on salinity and temperature show that the chl *a* maximum observed on day 149 is in the same position as 'Bottom Frontal Water', the characteristics of which are a mixture of 'Channel' and 'Central North Sea Bottom' waters (Fig. 7d; for more details see LI *et al.*, 1989).

5.2. JUNE 9-24 (DAYS 160-175) 1986

5.2.1. DESCRIPTION OF OBSERVATIONS

The chl *a* distribution observed after the NW-storm (Fig. 8) is generally found to be similar to the one observed on day 149; it resembles TB as depicted in Fig. 2, although its centre roughly overlies mooring B and its extent is limited at mooring F. TA is not observed, but it is noted that hardly any stations cover the area between moorings A and B. TA' is generally found from a single observation.

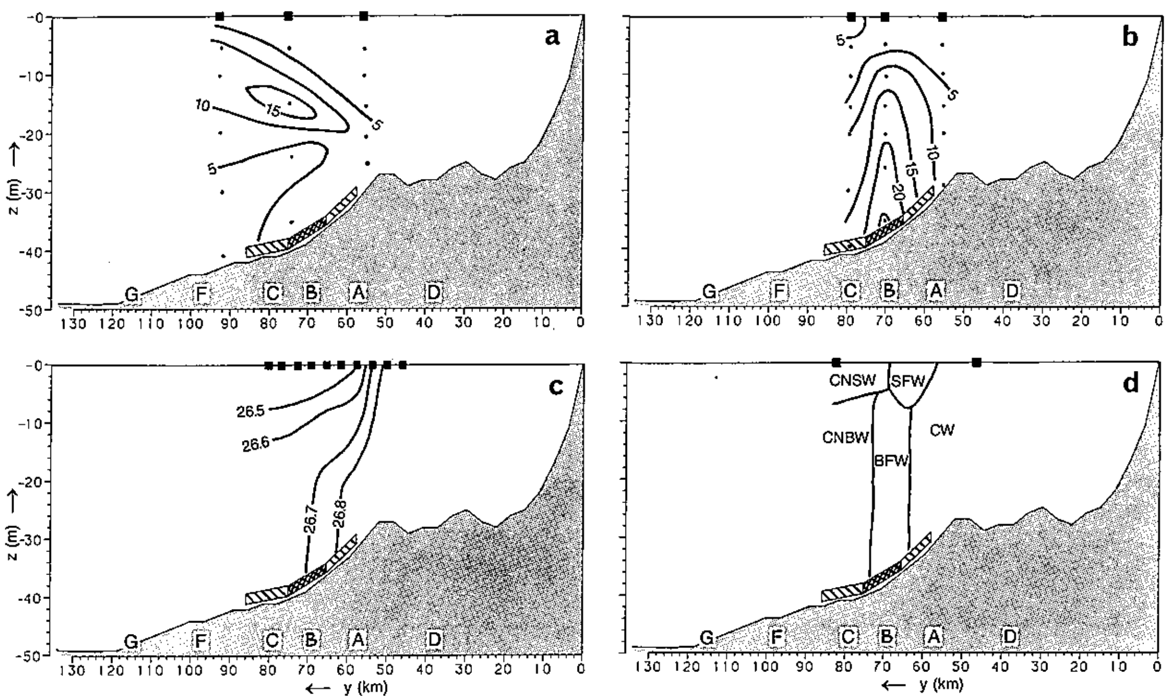

Fig. 7a. Distribution of chl *a* in mg m^{-3} in a vertical cross-isobath plane observed on day 146, 1986. b. Similar as Fig. 7.a but for day 149, 1986. c. Density anomaly in kg m^{-3} observed on day 149, 1986. d. Water mass distribution inferred from cluster analysis (LI *et al.*, 1989). CNSW = Central North Sea water; CNBW = Central North Sea bottom water; SFW = surface frontal water; BFW = bottom frontal water; CW = Channel water.

Generally, the area of large chl *a* amounts corresponds to the 'area' of large acid ratio values (R > 1.8) (Table 1), indicating that here chl *a* may be considered 'fresh'. HPLC cluster analysis shows that the large chl *a* amounts generally correspond to areas of one algal pigment cluster (Figs 8c and e).

The density distribution shows a frontal zone near mooring A, which strengthens during days 160-165. Between days 165-167 a 'Coastal Water' front is advected into the area by easterly winds. From day 167 onward only weak fronts are formed, always near mooring A. Cluster analysis on the CTD data between days 170-171 (Fig. 8d) reveals 'Bottom Frontal Water' in the narrow zone between isopycnals of $\sigma_t = 26.4$ kg m^{-3} near mooring A. Stratification gradually intensifies with time and the average pycnocline depth decreases from -8 to -15 m.

TABLE 1

Vertically averaged acid ratios for three positions in the vertical cross-isobath plane, indicted by mooring names. no=no observations

	y-position		
period	*A-D*	*B-F*	*F-G*
146	1.77 ± 0.04	1.84 ± 0.05	1.72 ± 0.05
148	1.73 ± 0.06	1.80 ± 0.04	no
160/161	1.66 ± 0.10	1.82 ± 0.06	no
163/164	1.70 ± 0.09	1.85 ± 0.05	no
170/171	1.72 ± 0.13	1.85 ± 0.03	no
182/183	1.6 ± 0.3	1.72 ± 0.16	1.6 ± 0.2

Except during day 175 (Fig. 8e) the general circulation pattern corresponds to wind-driven cross-isobath circulation (VAN HAREN, 1990b). However, the most conspicuous observation is the upwelling zone between moorings A and B, which seems to be fixed in cross-isobath position, irrespective of the direction of wind stress and of the sign of the cross-isobath density gradient. Although not always very clearly, some indication of the upwelling is reflected in locally upwardly bent isopycnals (Fig. 8).

5.2.2. HORIZONTAL AND VERTICAL ADVECTION

The chl *a* and density cross-sections shown in Fig. 8 are not exactly in the y-direction, but along N-S tracks. Mostly, data observed along 4°30′ E are used and, when these were not available, along N-S tracks between 4°20′ - 4°40′ E. It is assumed that isopleths of chl *a* are aligned along the isobaths (x-axis). Note that this corresponds more or less to the

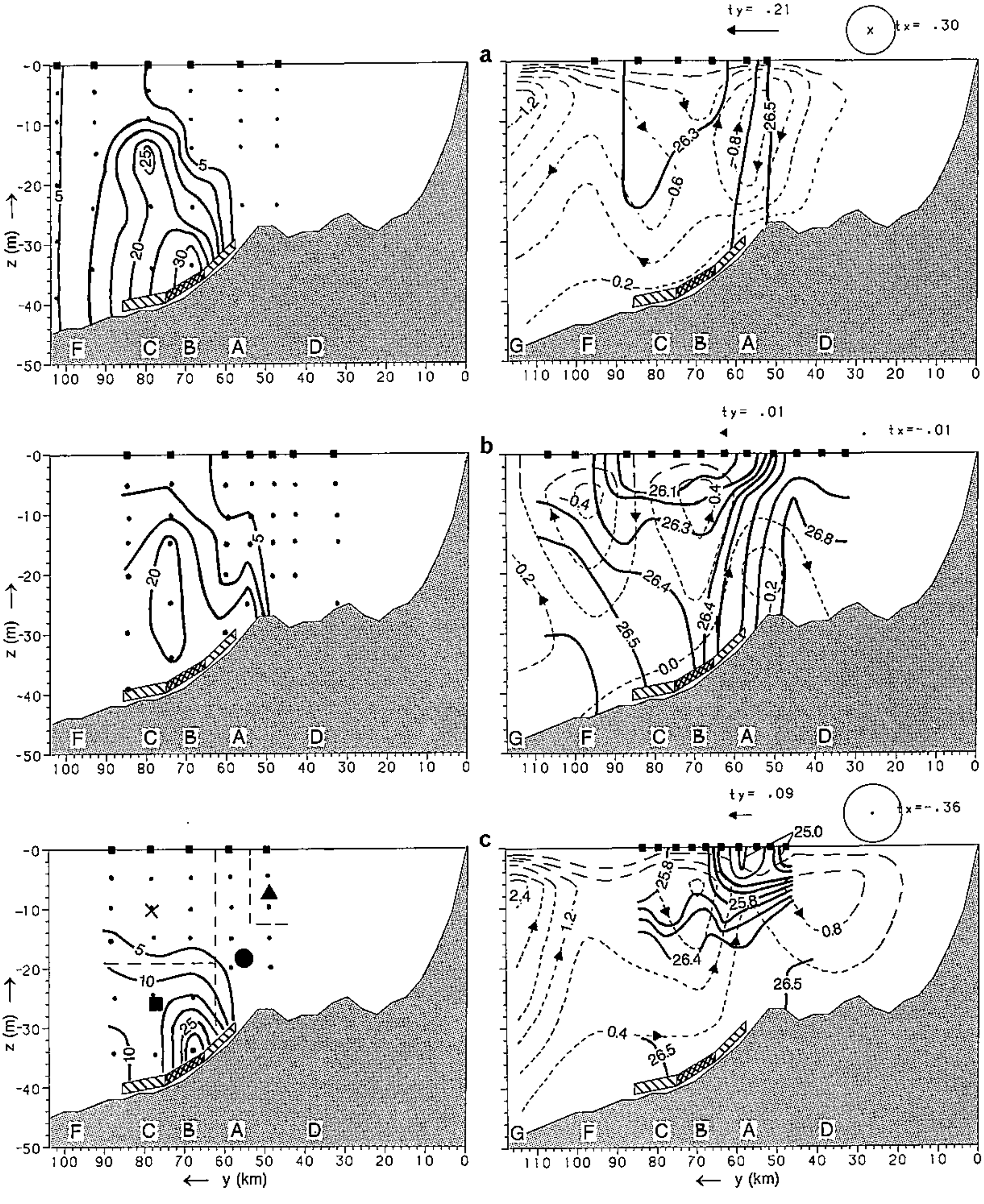

Fig. 8. For caption see opposite page.

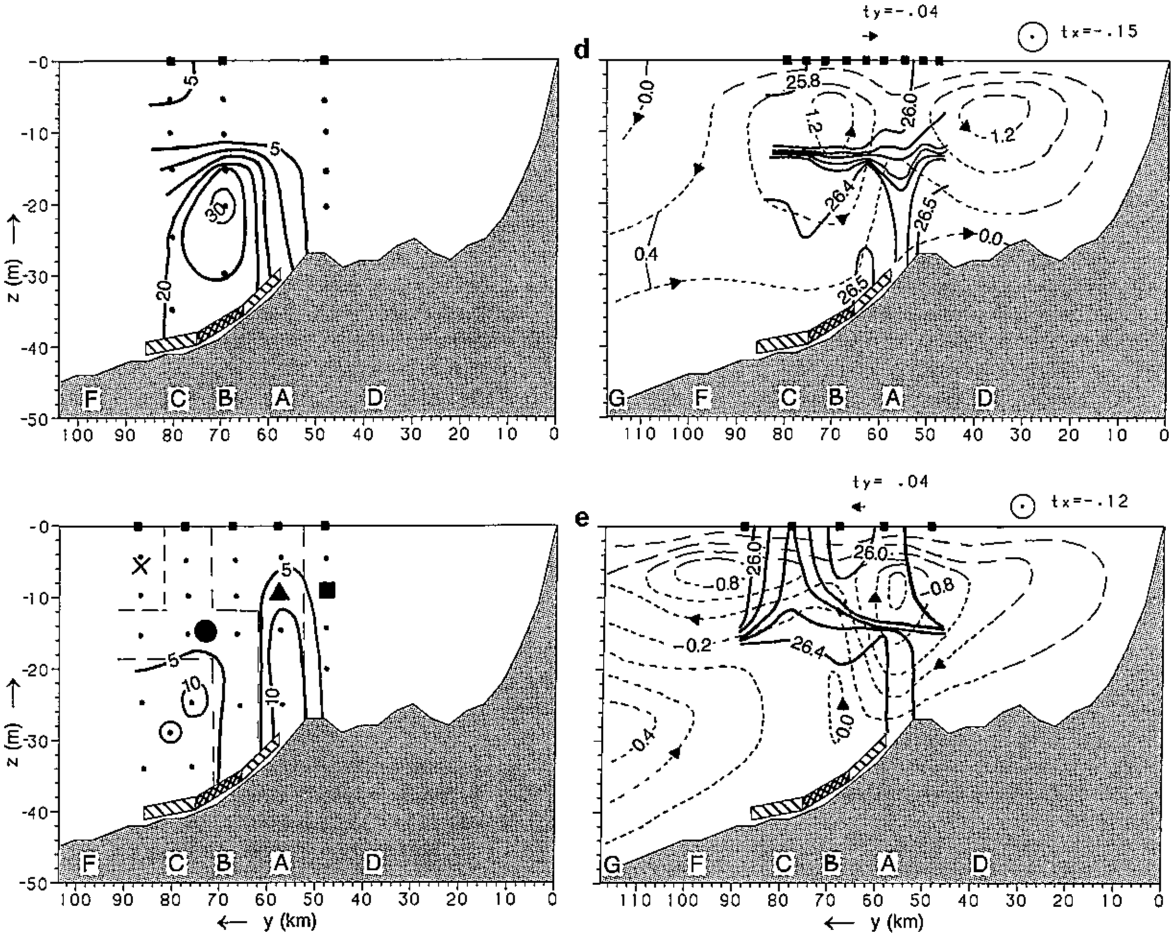

Fig. 8. Distributions of chl *a* ($mg\ m^{-3}$), density ($kg\ m^{-3}$) and water circulation ($m^2\ s^{-1}$) in a vertical cross-isobath plane in June 1986. On the left chl *a* distributions are shown. On the right the density distribution (solid) and the cross-isobath circulation (dashed) are shown. Long dashed streamlines (Ψ) have not been inferred from observations, but interpolated such that $\Psi = 0$ at the surface. Above each figure the wind stress component magnitudes (in $N\ m^{-2}$) and directions are shown. a. days 160-161; chl *a* transect along 4°40′ E b. days 163-164; chl *a* transect along 4°30′ E c. days 166-167; chl *a* transect along 4°15′ E. The large symbols indicate algal pigment clusters. d. days 170-171; chl *a* transect along 4°22′ E e. days 174-175; chl *a* transect along 4°30′ E. The algal pigment clusters which are indicated by symbols occurring in Fig. 8c do not have the same algal pigment composition.

horizontal distribution of turbidity, but that it does not correspond to the observations on bird counts and by echo-sounder, which do show non-zero response only over a finite distance in along-isobath direction.

As the quantitative information of the CZCS chl *a* images is unreliable and the along-isobath extent of the field observations is limited, we can only estimate a possible magnitude of the horizontal advection term by comparing it with other terms in (3). For $v << u$, $\partial C/\partial x$ can be estimated by assuming that the magnitude of $u\partial C/\partial x$ is equal to the magnitude of $w_s \partial C/\partial z$ ($w = 0$ here). From Fig. 8 we find an average $\partial C/\partial z = -0.6\ mg\ m^{-3}\ m^{-1}$ between the surface and the bottom. With $w_s \approx -0.5 \cdot 10^{-4}\ m\ s^{-1}$ and $u = 5\ cm\ s^{-1}$ we obtain $\partial C/\partial x \approx -0.6\ mg\ m^{-3}\ (km)^{-1}$, which implies that within 30 km an amount of 20 $mg\ m^{-3}$ should settle. Then, this hypothetical chl *a* gradient in the along-isobath direction would be similar in magnitude to the one observed in the cross-isobath direction. This seems unlikely. However, for the TA chl *a* maximum, observed by CREUTZBERG (1985), we deduce a value of $\partial C/\partial x = -0.07\ mg\ m^{-3}\ (km)^{-1}$, *i.e.* a chl *a* decrease along the isobaths of 3 $mg\ m^{-3}$ over 40 km, which seems possible.

Note that this is no proof: observations are lacking, but we may regard $u\partial C/\partial x$ as a possible relevant term in (3) for a TA chl *a* maximum. However, we assume that for the observations shown in Figs 7 and 8 vertical mixing and local generation are more important in (3) than this term.

5.2.3. VERTICAL MIXING AND SETTLING

We consider the chl *a* distribution between moorings B-C: a sub-surface maximum is found just below the pycnocline. From this maximum, the profile steeply decreases upwards and slowly decreases towards the bottom. This sub-surface maximum may be the result of settling of a near-surface bloom. If so, however, this settled bloom stays for quite some time at the base of the pycnocline (Figs 7 and 8).

In terms of generation, obviously nutrients originating from the enriched bottom are mixed with the overlying water column up to the pycnocline. If we assume that just below the pycnocline the light availability is high, a bloom may occur.

Like nutrients, the locally generated phytoplankton is subject to the vertical mixing regime, but this mixing must compete with the settling of the particles. Under the assumption that a complete balance between these two processes occurs, a quantification may provide a relative estimate of $(w+w_s)$ *versus* K_d from the chl *a* concentration profiles. We will then also be able to distinguish strong upwelling zones from downwelling zones from the profiles.

The balance referred to above is given by:

$$(w+w_s)\,\frac{\partial C}{\partial z}=K_d\,\frac{\partial^2 C}{\partial z^2} \qquad (7)$$

which we apply for $-h_2<z<-h_1$, a layer over which we may assume that K_d and $(w+w_s)$ are constant. We obtain:

$$\frac{C(z)-C(-h_1)}{C(-h_2)-C(-h_1)}=\frac{\exp(z/\alpha)-\exp(-h_1/\alpha)}{\exp(-h_2/\alpha)-\exp(-h_1/\alpha)}, \qquad (8)$$

with $\alpha = K_d/(w+w_s)$. Then, the sign of α can be immediately found from the position of the concentration profile with respect to a straight line connecting $C(-h_2)$ and $C(-h_1)$ (Fig. 9).

Several profiles investigated between the bottom and 20 m depth between C and B all showed negative α, the value of which was estimated as $\alpha = -25$ m. Some 'sensitivity' tests show that this value is correct within one order of magnitude. Surprisingly, with $w = 0\ \mathrm{m\,s^{-1}}$ between moorings B-C and with $w_s = -0.5\cdot10^{-4}\mathrm{m\,s^{-1}}$, we obtain $K_d \approx 1.2\cdot10^{-3}\ \mathrm{m^2\,s^{-1}}$, which is not too far off the value estimated from the current and density profiles (*i.e.* $K_d = 5\cdot10^{-3}\ \mathrm{m^2\,s^{-1}}$). No estimate can be given for the low-mixing pycnocline region, as data points are too few.

Only a few chl *a* concentration profiles have been obtained in the upwelling zone between moorings A-B (Fig. 8). Between days 160-161 at $y=56$ km for $-15<z<0$ m, $\alpha=2$ m is found. Between days 163-164 at $y=62$ km $\alpha=-35$ m for $-30<z<0$ m. Thus, the values of α do not yield a conclusive result, other than that indeed a positive value of α is found (once).

It may be concluded that with large uncertainties a local balance between vertical mixing and advection exists. This explanation is similar to the one given by CREUTZBERG (1985). Qualitative, let alone quantitative, evidence for an upwelling region between moorings A-B from vertical chl *a* concentration profiles is poor, but it is stressed that it is doubtful whether this region really has been covered by stations.

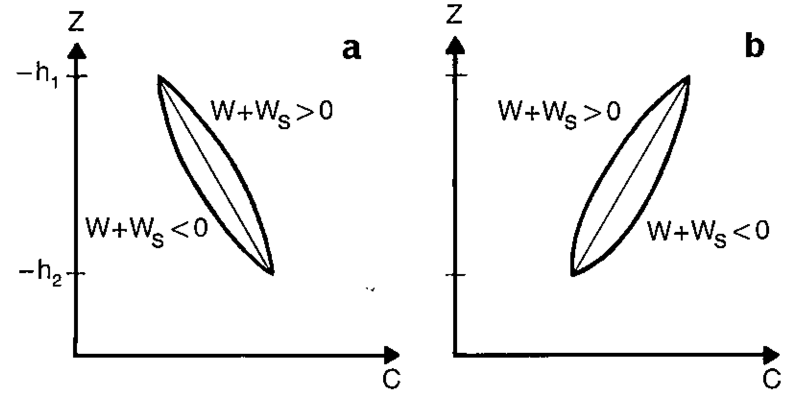

Fig. 9. Dependence of the sign of vertical velocity $(w+w_s)$ on the shape of theoretical vertical concentration (C) profiles according to (8), which indicates a balance between vertical mixing and settling between depths h_1 and h_2, between which eddy diffusivity and $(w+w_s)$ are assumed constant. a. $C(-h_1) < C(-h_2)$ b. $C(-h_1) > C(-h_2)$

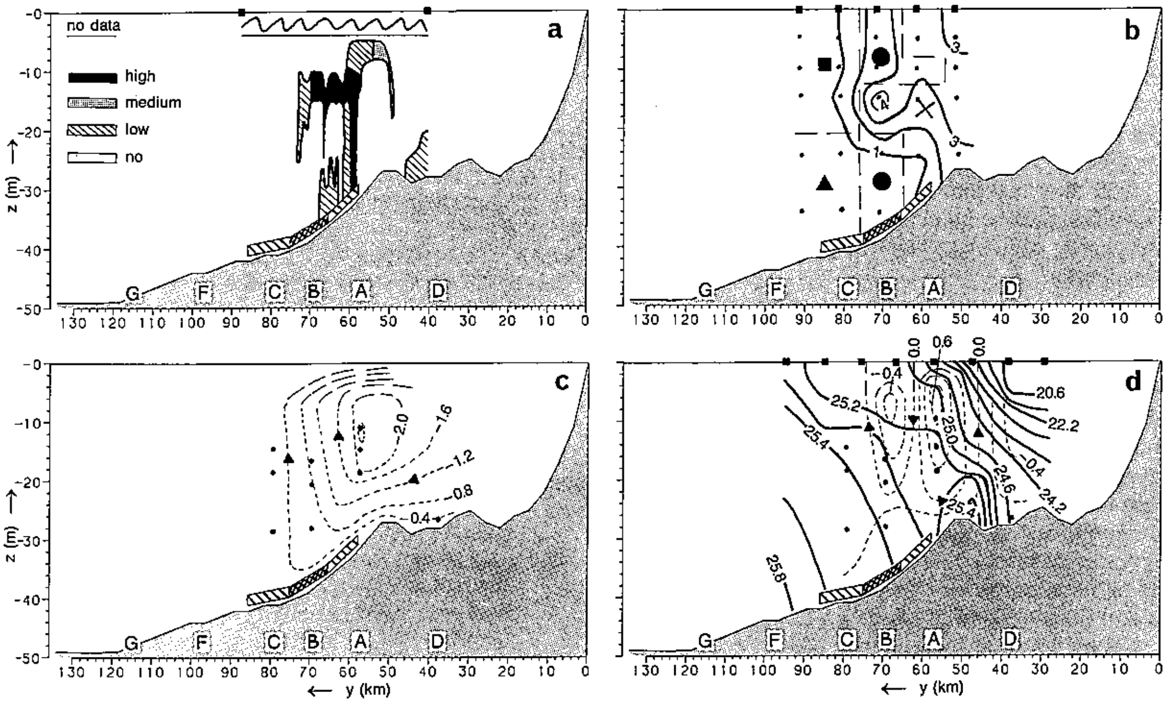

Fig. 10a. Interpretation in four grey tones of a scan of a 50 kHz echo-sounder of the trajectory indicated by the two solid squares. The scan was obtained between days 231.8-232.0, 1987. b. chl *a* distribution in mg m^{-3} and cluster results observed between days 234.5-235.0, 1987. c. Cross-isobath circulation in $m^2\ s^{-1}$ observed between days 230.5-231.0, 1987. d. Density distribution in kg m^{-3} observed along 4°30′ E between days 231.7-232.1, 1987 and cross-isobath circulation in $m^2\ s^{-1}$ observed between days 231.5-232.5, 1987.

5.3. ONE ECHO-SOUND SCAN

Indirect evidence for the existence of an intensified chl *a* maximum near mooring A has been provided by a strong acoustic response during one of the echo-sound scans obtained at the end of day 231, 1987. This scan shows an intense horizontal black band near 12 m depth and, near mooring A, a narrow band of a horizontal width of 2 km, which extends from the surface towards the bottom (Fig. 10a). The band at $z = -12$ m is found at the same depth as a weak pycnocline. A similar band at $z \approx -6$ m, between moorings A and D, follows the isopycnals which depict a strong density front. To a fair approximation the area occupied by non-zero response corresponds to the area with chl *a* >3 mg m^{-3} (Fig. 10b). Near mooring A also a weak near-bottom density minimum is observed (like between days 170-171, 1986).

Associated with the density front is a downwelling zone, observed between moorings A-B (which is rare) (Fig. 10d). For unexplained reasons, the day before the echo-sound and density observations were made, an intense upwelling between moorings A-C was observed (Fig. 10c). Note the small amount of current meters still operating at the time of these observations.

6. CONCLUSIONS

The observed chl *a* maximum overlies the extensive benthic zone consisting of large mud and POC contents and it extends from the bottom towards the pycnocline. The chl *a* maximum observed by Creutzberg (1985) was not found in 1986, partially because hardly any observations were obtained in the small region where this chl *a* maximum was found. An echo-sound scan, made in August 1987, however did show a large response over the total water column in an area of small cross-isobath extent of O (2 km) overlying the steepest bottom slope.

As far as has been observed, the chl *a* isopleths align with the isobaths. Observations during other periods on numbers of birds and by echo-sounder show non-zero response in a narrow band overlying the steepest bottom slope but appear to be of a finite extent in along-isobath direction.

Although not conclusive, horizontal advection of chl *a* is estimated to be small compared with vertical advection for the 1986 observations, but may be important for the observations made by CREUTZBERG (1985). The chl *a* distribution observed in 1986, considered as steady state, is roughly described by a local balance between vertical advection and mixing. The observed chl *a* is locally generated near the pycnocline, due to favourable conditions by mixing of nutrients with the overlying water. From the vertical chl *a* distribution no evidence is found for the upwelling zone, which has been inferred from current observations.

All in all, the region under consideration may be termed a transition in more than one respect. Not only does it contain a marked change in water depth with its associated features: a changing tidal current intensity and associated degree of turbulence; a related changing degree of sedimentation and a cross-isobath density front with its along- and cross-isobath circulation. It appears to be at a confluence of water masses too, which probably carry different types of nutrients. It is thus the unusual combination of circumstances not only in the vertical plane but also in the horizontal plane which appear to favour the food chain at this specific site.

7. REFERENCES

ABRAHAM, G., 1988. Turbulence and mixing in stratified flows. In: J. DRONKERS & W. VAN LEUSSEN. Physical processes in estuaries. Springer-Verlag, Berlin: 149-180.

BIENFANG, P.K., 1980. Phytoplankton sinking rates in oligotrophic waters off Hawaii., USA.—Mar. Biol. **61**: 69-77.

CREUTZBERG, F., 1985. A persistent chlorophyll *a* maximum coinciding with an enriched benthic zone. In: P.E. GIBBS. Proceedings of the nineteenth EMBS, Cambridge University Press, Cambridge: 97-108.

CREUTZBERG, F. & H. POSTMA, 1979. An experimental approach to the distribution of mud in the southern North Sea.—Neth. J. Sea Res. **13**: 99-116.

CREUTZBERG, F., P. WAPENAAR, G. DUINEVELD, N. LOPEZ LOPEZ, 1984. Distribution and density of the benthic fauna in the southern North Sea in relation to bottom characteristics and hydrographic conditions.—Rapp.-verb. Réun. Cons. int. Explor. Mer **183**: 101-110.

CSANADY, G.T., 1982. Circulation in the coastal ocean. Reidel Publishing Company, Dordrecht: 1-279.

CULLEN, J.J., 1982. The deep chlorophyll maximum: comparing vertical profiles of chlorophyll *a*.—Can. J. Fish. Aquat. Sci. **39**: 791-803.

EISMA, D. & J. KALF, 1987. Dispersal, concentration and deposition of suspended matter in the North Sea.—J. Geol. Soc. Lond. **144**: 161-178.

GARRETT, C.J.R. & J.W. LODER, 1981. Dynamical aspects of shallow sea fronts.—Phil. Trans. R. Soc. Lond. **A302**: 563-581.

HAREN, J.J.M. VAN, 1990a. Sub-tidal dynamics of a near-coastal zone in the North Sea.—Neth. J. Sea Res. **25**: 31-44.

——, 1990b. Observations on the horizontal and vertical structure of currents at sub-tidal frequencies in the central North Sea. Submitted for publ. in Neth. J. Sea Res.

HOLLIGAN, P.M., T. AARUP & S.B. GROOM, 1989. The North Sea: satellite colour atlas.—Cont. Shelf Res. **9**: 667-765.

LEOPOLD, M.F., 1988. A concentration of Guillemots (*Uria aalge*) at a tidal front near Texel, after the breeding season. In: M.L. TASKER. Seabird food and feeding ecology. Proc. 3rd Int. Conf. Seabird Group, Cambridge: 32-33.

LI, H., J.J.M. VAN HAREN & H.M. VAN AKEN, 1989. Cluster analysis as a method to discriminate water masses in shelf seas. ICES-paper Hydrography Committee C.M. 1989/C:3:1-14.

LODER, J.W. & T. PLATT, 1985. Physical controls on phytoplankton production at tidal fronts. In: P.E. GIBBS. Proceedings of the nineteenth EMBS, Cambridge University Press, Cambridge: 3-21.

MAAS, L.R.M. & J.J.M. VAN HAREN, 1987. Observations on the vertical structure of tidal and inertial currents in the central North Sea.—J. Mar. Res. **45**: 293-318.

MCCAVE, I.N., 1984. Size spectra and aggregation of suspended particles in the deep ocean.—Deep Sea Res. **31**: 329-352.

PINGREE, R.D. & D.K. GRIFFITHS, 1978. Tidal fronts on the shelf seas around the British Isles.—J. Geophys. Res. **83**: 4615-4622.

——, 1980. Currents driven by a steady uniform wind stress on the shelf seas around the British Isles.—Oceanol. Acta **3**: 227-236.

PRANDLE, D., 1984. A modelling study of the mixing of ^{137}Cs in the seas of the European Continental Shelf.—Phil. Tans. R. Soc. Lond. **A310**: 407-416.

SIMPSON, J.H., D.J. EDELSTEN, A. EDWARDS, N.C.G. MORRIS & P.B. TETT, 1978. The Islay front: physical structure and phytoplankton distribution.—Est. coast. mar. Sci. **9**: 713-726.

SMETACEK, V., K. VON BROECKEL, B. ZEITSCHEL & W. ZENK, 1978. Sedimentation of particulate matter during a phytoplankton spring bloom in relation to the hydrographical regime.—Mar. Biol. **47**: 211-226.

(received 12 March 1990; revised 29 May 1990)